RSC Advances

ROYAL SOCIETY OF CHEMISTRY

www.rsc.org/advances

Synthesis and characterization of molecularly imprinted polymer embedded composite cryogel discs: Application for the selective extraction of cypermethrins from aqueous samples prior to GC-MS analysis

Huma Shaikh[1], Müge Andaç[2], Najma Memon[1], Muhammad Iqbal Bhanger[3], Shafi Muhammad Nizamani[1], Adil Denizli[4*]

[1]National Center of Excellence in Analytical Chemistry, University of Sindh, Jamshoro 76080, Pakistan.
[2]Department of Environmental Engineering, Hacettepe University, Ankara, Turkey
[3]H. E. J. R.I.C., I.C.C.B.S. University of Karachi, Karachi -75270, Sindh, Pakistan.
[4]Department of Chemistry, Biochemistry Division, Hacettepe University, Ankara, Turkey

ABSTRACT

Molecularly imprinted partricles embedded composite cryogel discs specific for α-cypermethrin and β-cypermethrin were prepared. Two different types of imprinted particles were embedded into cryogel to prepare composite cryogel specific for two isomers of cypermethrin simultaneously. Adsorption studies revealed that MIP is extremely selective for α-cypermethrin and β-cypermethrin with outstanding adsorption capacity. A sensitive analytical method comprising of MISPE coupled with GC-MS has been developed to quantify trace levels of α-cypermethrin and β-cypermethrin in real water matrices. The polymer showed fast kinetics and follows Pseudo-second-order kinetic model very well (R^2 = 0.9999). It shows excellent capacity towards α-cypermethrin and β-cypermethrin with higher total number of binding sites (N_t=96 μmol g^{-1} for α-cypermethrin and 95 μmol g^{-1} for β-cypermethrin). The MIP showed selectivity over the homologues of α-cypermethrin and β-cypermethrin with imprinting factor (IF) 11.2, 10.0, 1.04 and 1.20 for α-cypermethrin, β-cypermethrin, deltamethrin and permethrin, respectively. The developed MISPE method followed by GC-MS enhanced the sensitivity and selectivity of assay. This method was successively applied on the samples of lake water for the determination of α-cypermethrin and β-cypermethrin simultaneously. Moreover, the synthesized MIP can be easily regenerated and repeatedly used without lose of efficiency.

Keywords: Molecularly imprinted polymers; Cryogel; SPE, Cypermethrin; GC-MS.

Corresponding Author: Prof. Adil Denizli, email: denizli@hacettepe.edu.tr

Co-corresponding Author: Dr. Najma Memon, email: najmamemon@gmail.com

Author: Huma Shaikh, email: huma_hashu@gmail.com

Co-authors:

Dr. Muge Andac, email : andac@hacettepe.edu.tr

Prof. Muhammad Iqbal Bhanger, email: dbhanger2000@gmail.com

Prof. Shafi Muhammad Nizamani, email: drshafi.nizamani@gmail.com

1. Introduction

Synthetic pyrethroids (SPs) are one of the most chiral pesticides due to the presence of 2 or 3 stereogenic centers in their chemical structure. Consequently, almost every SP has 2 or 4 enantiomer pairs, or 2 or 4 diastereomers. SPs are extensively utilized as insecticides on animals, crops and in households. As the carbamates are being restricted increasingly the SPs may find their way to be used as organophosphate insecticides. SPs are acutely toxic to fish and aquatic invertebrates [1].

One of the broadly used pyrethroid is Cypermethrin (CYP) that has been used extensively against pests in China and other countries for past 30 years. It is effective to control Lepidoptera, cockroaches and termites [2]. The insecticide is a mixture of its alpha (α), beta (β) and theta (θ) forms. β-CYP has lower activity than α-CYP but higher than other CYPs [3]. CYP found its broader use in agricultural crops, forests and public and animal health because it was considered safe [4], but there are increasing verifications that CYP is toxic to humans and animals when encountered consistently or in high doses. CYP can accumulate in body fat, skin, liver, kidneys, adrenal glands, ovaries, lung, blood, and heart of mammals [5-7]. CYP mainly targets the central nervous system. Moreover, high doses of CYP can cause twitching, drowsiness, coma, and seizures in humans [8]. The neurotoxic effect of CYP is exerted via voltage-dependent sodium channels and integral protein ATPases in the neuronal membrane [9-10]. The reproductive organs are also affected by the toxicity of CYP [11-12]. Studies carried on male mice proposed that CYP reduces the weight of testosterone-sensitive organs, enhances the height of seminal gland epithelium, and decreases sperm count and motility [11, 13-15]. The mechanism through which male reproduction is affected by CYP is not clear. Although, it metabolizes quickly in mammals numerous studies revealed that CYP damages the brain, liver, and erythrocytes by causing oxidative stress [16-19].

Usually, the pyrethroid insecticides are determined by using gas chromatography coupled with electron-capture detection (GC-ECD), mass spectrometry (GC-MS), or liquid chromatography-electrospray ionization mass spectroscopy (LC-MS) [20-22]. However, complicated matrices may lead to the positive errors while analysis. Therefore, it is essential to remove coextracted matrix of interference and improve the selectivity of method by introducing clean-up steps before analysis. Numerous pretreatment methods such as solid phase extraction (SPE) [23], stir bar sorption extraction (SBSE) [24], liquid-phase microextraction (LPME) [25], solid-phase

microextraction (SPME) [26], and liquid-liquid extraction have been broadly applied. Nevertheless, lengthy equilibrium times and strict experimental control required by SBSE, LPME, and SPME **limit** their applications on large-scale analysis [24-27]. Although, liquid-liquid extraction is an affective extraction technique for water samples but its applications are limited due to the formation of emulsions [28]. Thus, solid phase extraction based on molecularly imprinted polymers (MISPE) has been used more effectively for the isolation and clean-up of SPs from different matrix samples [29-33]. Therefore, MIPs are proved to be a better choice of selective pre-concentration methods. Vonderheide *et al.,* [29] reported MISPE method for determination of cypermethrin and cyfluthrin in composite diets using GC-MS. This method showed good percent recoveries of cypermethrin from food samples. A method based on MISPE-GC-ECD was also reported for simultaneous determination of six pyrethroids including cypermethrin and deltamethrin. Although the method shows good detection and quantification limits but MISPE cartridges were conditioned with organic solvents [30], which is a drawback of using traditional methacrylate polymer backbone.

MIPs can be used for capturing organic molecules that appear as pollutants in water. A problem with MIPs is that they are composed of tight polymer material with very small pores. Therefore, MIPs are used as small particles so that many binding sites are exposed to the surface. On the other hand, it becomes problematic to handle these small structures and, when packed in columns, massive back-pressures are built up. Thus, a composite with the MIP particles immobilized in a cryogel offers an attractive arrangement because good accessibility is offered by the cryogel and low back-pressure is maintained. Embedding MIP particles in the polymer network of a cryogel is attractive. The gel offers large pores with convective flow and thus good mass transfer conditions, and the MIPs represent the affinity binders [34-36]. When characterizing such preparations, one has to study selectivity, capacity, and ability to regenerate [37]. Thus composite cryogels embedded with MIP particles are the most eligible candidates for extraction due to their high compatiblity with aqueous as well as biological systems. They are also resistant to a broad range of buffer systems which ultimately adds to their credibility. Moreover, composite cryogels possess high toughness and superfast **response** that make extraction process robust and quick [38-39].

In the present study, we are reporting composite cryogel discs embedded with MIP particles selective for α-CYP and β-CYP. The composite cryogel discs were successfully employed for

enhanced and efficient pre-concentration of α-CYP and β-CYP through solid phase extraction technique prior to GC-MS detection. The synthesized MIP embedded composite cryogel discs were characterized thoroughly and examined for their adsorption capacity, selectivity and reusability. The developed MISPE method was validated thoroughly and found robust and highly sensitive to low limits of detection for α- and β-CYP.

2. Experimental

2.1. Materials

All solvents/reagents used for the synthesis and preparations of solutions were of analytical grade. Ethanol, methanol, acetic acid, cyclohexane, toluene, ether, ethyl acetate, and dichloromethane were purchased from Fisher Scientific, UK. α-cypermethrin, β-cypermethrin, deltamethrin, permethrin, L-phenylalanine, sodium nitrite ($NaNO_2$), potassium carbonate (K_2CO_3), 2-hydroxyethyl methacrylate (HEMA), ethylene glycol dimethacrylate (EGDMA), poly (ethylene glycol) diacrylate (PEGDA), tetramethylethylenediamine (TEMED), methacryloyl chloride and ammonium persulphate (APS) were obtained from Sigma-Aldrich, Germany.

The deionized water purified by a Millipore Milli-Q Plus water purification system (Elga model classic UVF, UK) was used to prepare aqueous solutions

2.2. Preparation of α- and β-CYP imprinted particles embedded composite cryogel discs

2.2.1. Synthesis of N-methacryloyl-L-phenylalanine (MAPA) monomer

In the synthesis of CYP imprinted polymer, MAPA was used as functional monomer. N-methacryloyl-L-phenylalanine (MAPA) was synthesized by following the elsewhere reported method [40]. Precisely, the mixture of L-phenylalanine (5.0 g) and $NaNO_2$ (0.2 g) was prepared by dissolving them in 30 mL of K_2CO_3 aqueous solution (5%, w/v). The mixture was maintained at 0 °C followed by gradual addition of methacryloyl chloride (4.0 mL) under gentle nitrogen stream. The reaction was continued for 2 h with constant magnetic stirring. Finally, the pH of reaction solution was maintained at 7.0 at the completion of reaction. The product was extracted using ethyl acetate and aqueous phase was removed using rotary evaporator. To crystallize the residue (MAPA) ether-cyclohexane mixture was utilized.

2.2.2. Synthesis of α- and β-CYP imprinted particles embedded composite cryogel discs

The α- and β-CYP imprinted monoliths were prepared separately and were embedded together in composite cryogel discs. The α- and β-CYP imprinted monolith was synthesized by preparing complexation mixture of α- and β- CYP (0.0416 g) and MAPA ($5x10^{-4}$ g) in 200 µL of ethanol which was then poured into a glass tube containing toluene (1 mL), HEMA (2 mL) and EDGMA (1 mL). The polymer mixture was purged with pure nitrogen gas and then APS (0.02 g) was added. The polymerization was assisted by addition of TEMED (100 µL) and carried out at room temperature for 24 h. After completion of polymerization the monolith was removed from glass tube and thoroughly washed with 9:1 mixture of methanol/acetic acid and 100% methanol. The complete removal was confirmed by analyzing the washes on GC/MS. The air dried monolith polymer was ground and sieved using different ranges of sieve size. Polymer particles smaller than 20 µm were selected for embedding.

200 mg of each α- and β-CYP imprinted particles of mentioned range were dispersed in D.I water (13.6 mL) for 30 min. HEMA (1.3 mL) and PEGDA (0.51 mL) were added to the particles solution and mixture was cooled enough in refrigerator but not allowed to freeze. APS (185 µL from 10% stock solution, 1% w/v) and TEMED (18.5 µL, 1% w/v) were added in the above mixture maintained at 0 °C in an ice bath. Immediately, the reaction mixture was poured between two glass plates separated by 1.5 mm thick spacers. The polymerization solution between the plates was frozen at -16 °C for 24 h and then thawed at room temperature. The resulting cryogel sheet was cut into circular pieces (0.5 cm diameter) with a perforator. The MIP particles embedded composite cryogel discs were washed several times with water to remove non-reacted monomers and to check leaching of particles. **Non-imprinted polymer (NIP)** particles embedded composite cryogel discs were also synthesized following the same procedure but in the absence of the **templates.**

2.3. Characterization

Thermo Nicollet AVATAR 5700 FT-IR spectrometer was used to record FT-IR spectra of α- and β-CYP imprinted composite cryogel discs through KBR pellets. JEOL JSM-6380 scanning electron microscopy (SEM) was utilized to perform surface characterization of composite cryogel discs.

2.4. Chromatographic determination of CYPs

In all instances aqueous solutions containing CYPs were extracted with equal volume (single extraction) of dichloromethane and 1μL of extract was injected onto GC-MS using splitless mode. Similar procedure was adopted for constructing calibration graphs, sorption studies and samples analysis, however the non-aqueous solutions containing CYPs were injected in GC-MS soon after filtration or preconcentration. The chromatographic system was consisted of a Thermo Scientific DSQ™ II Series Single Quadrupole GC-MS. It was installed with 30 meter HP-5MS column having I.D. 0.250 mm (Narrow bore) and film thickness of 0.25 μm. Helium was used as carrier gas. The calibration curves of CYPs were obtained at column temperatures from 100 °C to 300 °C at 10 °C min^{-1} (keeping this temperature for 10 min). The temperatures of injector and detector were 300 °C and 350 °C, respectively.

2.5. Swelling studies

To estimate the gelation yield, swollen MIP composite cryogel disc was dried at 60 °C in an oven. The drying was continued till the constant weight of MIP composite cryogel disc was achieved. The weight of dried sample (m_{dried}) was measured. The gel fraction yield was calculated as (m_{dried}/m_t) x100%, where m_t was the total mass of the monomers in the feed mixture. The samples of swollen gels (1 disc) were sucked dry on filter paper and then weighed ($m_{wet\ gel}$) to evaluate the swelling degrees of MIP composite cryogel. Finally, the weight of dried samples ($m_{dry\ gel}$) was obtained by drying them at **60 °C.** The degree of swelling was calculated as:

$$S_{w/w} = (m_{wet\ gel} - m_{dry\ gel})/m_{dry\ gel} \quad (1)$$

The rough estimation of total volume of macropores in the swollen cryogel disc was done as follows,

$$(m_{swollen\ gel} - m_{squeezed\ gel})/m_{swollen\ gel} \times 100\% \quad (2)$$

where ($m_{squeezed\ gel}$) is the weight of sample obtained after squeezing the free water from the swollen gel matrix.

The swollen gel weight percent was also estimated as:

184 $(m_{swollen\ gel} - m_{dried})/m_{swollen\ gel} \times 100\%$ (3)

185 All measurements were done in triplicate and the average values are presented.

186 **2.6. Sorption studies**

187 To evaluate the binding kinetics of α- and β-CYP imprinted composite cryogel discs 5 mL of 20
188 μg mL^{-1} α- and β-CYP solution in CH_2Cl_2 was added into nine separate 25 mL glass flasks
189 containing 1 polymer disc, which were then shaken (100 rpm) for 5, 10, 15, 20, 25, 30, 45, 60
190 and 120 minutes at room temperature. Subsequently discs were removed and mixtures were
191 analyzed as given in Section 2.4. The binding kinetics of non-imprinted composite cryogel discs
192 was evaluated using same methodology. The triplicate data were reported as the mean ± standard
193 deviation (S.D.).

194 For the estimation of adsorption capacity, 20 mL solution with various concentrations of CYPs
195 from 1 to 100 μg mL^{-1} in CH_2Cl_2 were introduced to 25 mL glass flasks containing single MIP
196 composite cryogel disc. The mixtures were shaken for 20 min with shaking speed of 100 rpm on
197 orbital shaker at room temperature to facilitate the adsorption of α and β cypermethrin onto the
198 MIP composite cryogel disc. All solutions were analyzed as given in section 2.4. The data were
199 obtained in triplicate and reported as the mean ± standard deviation (S.D.).

200 **2.7. Selectivity experiments with homologues of CYP**

201 Competitive recognition studies were performed with α- and β-CYP and other homologues .i.e.
202 deltamethrin and permethrin. 20 mL of α-CYP, β-CYP, deltamethrin and permethrin solution in
203 CH_2Cl_2 with initial individual concentrations of 20 μg mL^{-1} was introduced to MIP and NIP
204 composite cryogel discs. The mixtures were shaken for 20 min at room temperature, decanted
205 and investigated by GC-MS as described in the section 2.4. The data were obtained in triplicate
206 and reported as the mean ± standard deviation (S.D.).

207 **2.8. MISPE experiments**

208 To evaluate suitable pH for maximum binding of CYPs on MIP composite cryogel disc in
209 aqueous solutions, 100 mL of α- and β-CYP solutions (10 μg L^{-1}) maintained at pH ranging from
210 1.0 to 9.0 using phosphate buffers were shaken gently for 20 min at room temperature. Sample

after adsorption was decanted off and finally 5 mL methanol was used to desorb cryogel disc. The mixtures were shaken gently for 20 min at room temperature. The extract was evaporated till dryness under gentle stream of nitrogen and reconstituted in 0.5 mL CH_2Cl_2. The final extract was analyzed on GC-MS as explained in section 2.4.

200 mL of synthetic wastewater maintained at pH 7.0 spiked with α- and β-CYP at various concentrations was introduced to MIP composite cryogel disc. The mixtures were shaken for 20 min at room temperature, synthetic wastewater was decanted off and finally 5 mL methanol was used to desorb cryogel disc. The mixtures were shaken gently for 20 min at room temperature. The extract was evaporated till dryness under gentle stream of nitrogen and reconstituted in 0.5 mL CH_2Cl_2. The final extract was analyzed on GC-MS as explained in section 2.4. Synthetic wastewater sample was prepared by the method as reported earlier [41].

2.8.1. Validation study

For the validation of proposed MISPE procedure, the selectivity, linearity, sensitivity, precision, accuracy and detection and quantification limits were evaluated thoroughly. This study was performed on synthetic wastewater samples spiked with α- and β-CYP to provide samples containing concentration range of $1x10^{-4}$ to 10 μg L^{-1}. In order to optimize linearity and sensitivity of method the calibration curve was established via triplicate analysis of CYP spiked synthetic wastewater samples. The coefficient of determination (R^2) obtained from the calculation of regression line by least squares method demonstrated linearity whereas slope was used to demonstrate sensitivity of method.

Three different concentrations i.e. low, medium, and high (0.3, 1.0, and 4.0 μg L^{-1}, respectively) were selected to carry precision studies. For the assessment of intra-assay precision five replicates of each concentration were performed on the same day. However, for interpretation of interassay precision three replicates of each concentration were done on three different days. The percent relative standard deviation was calculated for replicates to expess precision. Various solvents checked to enhance extraction efficiency were, ethanol, methanol, acetic acid, acetonitrile and dichloromethane and their % recoveries were found to be 70, 95, 60, 65 and 55%, respectively.

The lake water samples were spiked with three different concentrations: 0.3, 1.0, and 4.0 μg L^{-1} and their triplicate analyses were performed to demonstrate accuracy of proposed method.

For optimizing limit of detection and limit of quantification, signal-to-noise ratios of 3 and 10 were used, respectively. The ratios were approximated at the retention time of the corresponding analyte peak.

2.9. Regeneration and reuse of polymer

MIP composite cryogel discs were regenerated and reused for 10 times. After every experiment, discs were collectively washed with 30 mL of ethanol for 1 h and then with 30 mL of methanol for 1 h. After washing with organic solvents, discs were washed with excess of D.I water and stored in it before further use.

3. Results and discussion

3.1. Synthesis of α- and β-CYP imprinted composite cryogel discs

Two different types of imprinted particles were embedded in cryogel discs to prepare composite cryogel specific for two isomers of CYP simultaneously with increased surface area and improved adsorption capacity. Embedding MIP particles in the polymer network of a cryogel is an attractive methodology for the extraction of samples because the large pores offered by cryogels permit convective flow and good mass transfer conditions, whereas the MIPs play the role of affinity binders efficiently [35, 42-43]. Thus, keeping in mind the double benefits of imprinted composite cryogels α- and β-CYP imprinted poly (hydroxyethyl methacrylate- N-methacryloyl-L-phenylalanine) monoliths were synthesized separately, washed, crushed, sieved and finally embedded in cryogel membrane. Two different types of particles were embedded to make MIP composite cryogel discs specific for both α- and β-CYP simultaneously. MAPA was chosen as functional monomer because additional interactions were expected between phenyl groups of MAPA and CYP. In order to assure the specificity of composite cryogels for both α- and β-CYP monoliths were prepared separately. The size of particles chosen for embedding in this study was < 20 μm. The reason of choosing smaller particles was to implant particles well in membrane of cryogel and to offer greater surface area to the template molecules. Also to embed more amounts of particles it was necessary to choose small particles. **The aim of this synthesis strategy was to devise MIP that is extremely selective for two isomeric compounds simultaneously. This is**

why at present only α- and β-CYP were selected as template molecules and θ-CYP was not included in the study. Furthermore, α and β-CYP were chosen on priority bases because they have higher activity than other CYPs [3]. The obtained results were satisfactory and may lead to synthesis of MIPs that are simultaneously selective for two or more compounds. Finally, the composite cryogel membrane was made by embedding two different imprinted particles and membrane was cut into discs. Hence, the MIP composite cryogel discs specific for α- and β-CYP were prepared. This scheme improves the adsorption capacity as well as selectivity of cryogel and leads to highly water compatible, robust, environmental friendly and biodegradable molecularly imprinted polymer specific for α- and β-CYP. Recently, Ma and Chen [44] have reported acrylate based MIP for selective extraction of pyethroid pesticides from fruit matrices. The synthesis method included encapsulation of magnetic carbon nanotubes with MIP to accomplish desired surface area. Shi *et al.,* [30] also reported molecularly imprinted solid phase extraction of pyrethroid pesticides from aquaculture seawater. Though, compatibility of cryogels with aqueous sytems is better than MIPs based on acrylate backbone. The cyclodextrin based MIP was reported by Guo *et al.,* [45] for selective extraction of pyrethroid pesticides from aqueous media. However, the values of imprinting factor revealed that MIP has limited specificity. The schematic representation of imprinting of CYP in poly (hydroxyethyl methacrylate- N-methacryloyl-L-phenylalanine) is shown in Fig. 1. The photographic image of MIP composite cryogel discs is also shown in Fig. 2.

3.2. Characterization

3.2.1. FT-IR spectra

The synthesized α- and β-CYP imprinted poly (hydroxyethyl methacrylate-N-methacryloyl- L-phenylalanine) particles and non-imprinted particles were characterized through FT-IR. Fig. 3 reveals FT-IR spectra of (a) α-CYP imprinted particles (b) β-CYP imprinted particles and (c) non-imprinted particles. Fig. 3 a, b and c reveal a sharp band due to C=O stretching at 1716, 1725 and 1704 cm^{-1}, respectively that indicates the presence of monomers in all polymers, it also reveals that C=O stretching shift from 1704 cm^{-1} (NIP) to 1716 cm^{-1} in α-CYP imprinted particles and to 1725 cm^{-1} in β-CYP imprinted particles. This may be due to different interactions of MAPA in all three polymers, it also proves that in MIP particles interactions between template molecule and monomers exist. All polymers reveal a prominent peak at 3401 cm^{-1} (NIP), 3434

298 cm^{-1} (α-CYP imprinted particles) and 3425 cm^{-1} (β-CYP imprinted particles) due to –OH
299 stretching. These peaks confirm polymerization as well as shifts in MIP particles revealed
300 interaction of –OH groups with template molecules. C-N stretching can be observed in the region
301 of 1150 cm^{-1} in all three polymers. However, significant shifts can be observed in C-O stretching
302 between carbon and hydroxyl groups i.e. 1021 cm^{-1} for NIP particles, 1038 cm^{-1} for α-CYP
303 imprinted particles and 1015 cm^{-1} for β-CYP imprinted particles. This is another sign of
304 interaction of –OH groups of monomer with template molecules. Aromatic C-H bending is
305 observed in NIP at 859 and 764 cm^{-1}, however these bending vibrations are shifted to 844 and
306 750 cm^{-1} in case of α-CYP imprinted particles and to 835 and 755 cm^{-1} in case of β-CYP
307 imprinted particles. These shifts of C-H bending vibrations indicate interaction of phenyl group
308 of MAPA with phenyl group of CYP. These FTIR spectra show that α- and β-CYP interact with
309 hydroxyl and phenyl groups of MAPA.

310 **3.2.2. SEM**

311 The SEM images of the CYP imprinted poly (hydroxyethyl methacrylate-N-methacryloyl- L-
312 phenylalanine) particles embedded MIP composite cryogel are shown in Fig 4. The particles
313 used for this study were sieved through 20 μm sieve. Particles smaller than 20 μm size were
314 chosen for embedding in membrane. Fig. 4a shows cross-sectional image of MIP composite
315 cryogel disc, it reveals that surface of disc is smooth where as inner thin walls are macroporous
316 and particles are embedded in them. A closer look to the walls of MIP composite cryogel (Fig.
317 4e) reveals that particles are embedded homogenously in the walls of cryogel. However, large
318 continuous interconnected pores (10–100 μm in diameter) that provide channels for the mobile
319 phase to flow through are still present and can be seen in Fig. 4a-f. These pores are an advantage
320 for adsorption studies as they allow the template molecules to access the specific binding sites
321 present in embedded particles. Baydemir *et al.,* [46] also reported similar results when embedded
322 bilirubin imprinted particles in cryogel.

323 **3.2.3. Swelling studies**

324 Swelling studies of composite cryogel discs were performed in water. The equilibrium swelling
325 degree of the MIP composite cryogel and NIP composite cryogel were found 8.4±0.31 g H_2O/ g
326 cryogel and 6.6±0.1 g H_2O/ g cryogel, respectively. The total volume of macropores in the

swollen composite cryogel was roughly estimated as 80±0.5 % and 73±0.3 % in MIP and NIP composite cryogel, whereas percent of swollen gel weight was estimated as 88.1±0.4 % and 84.8±0.35 % for MIP and NIP composite cryogel, respectively. MIP composite cryogel disc was opaque, spongy and elastic. It could be easily compressed by hand to remove water accumulated inside the pores. When the compressed cryogel disc was submerged in water, it soaked in water and within 1-2 s restored its original size and shape.

3.3. Sorption studies

3.3.1. Uptake kinetic studies

The adsorption kinetics of α- and β-CYP mixture onto MIP and NIP composite cryogel is presented in Fig. 5. The kinetic studies were performed by shaking 20 mL of α- and β-CYP solution (20 μg mL^{-1}) prepared in CH_2Cl_2. The results showed that the MIP composite cryogel had fast uptake kinetic for both α- and β-CYP and the binding equilibrium was almost reached within 20 min. The property of rapid adsorption kinetics of the MIP composite cryogel is an advantage for SPE application. Moreover, the imprinted composite cryogels reveal faster kinetics as compared to previously reported pyrethroid pesticides selective MIPs [45].

The pseudo-second-order kinetic model was used to describe the adsorption process,

$$\frac{t}{q_t} = \frac{1}{kq_e^2} + \frac{t}{q_e}, \quad (4)$$

where, k is the rate constant of second-order sorption (mg g^{-1} min^{-1}) and q_t is the adsorption capacity at any time (mg g^{-1}). From the equilibrium, t/q_t versus t is plotted in Fig. 6 the coefficients of determination (R^2) were 0.9999 for both α- and β-CYP and the q_e values (18.42 mg g^{-1} for α-CYP and 18.25 mg g^{-1} for β-CYP) obtained from the pseudo-second-order kinetic model were very closed to the q_e values (18.4 mg g^{-1} for α-CYP and 18.3 mg g^{-1} for β-CYP) obtained from experiment. This indicated that the adsorption of the MIP composite cryogel towards α- and β-CYP follows the pseudo-second-order kinetic model very well.

3.3.2. Static adsorption capacity of MIP and NIP composite cryogel discs

To investigate the affinity of α- and β-CYP imprinted MIP and NIP composite cryogel discs, a steady-state binding method and subsequent Scatchard and LF analysis were carried out. The binding isotherms of α- and β-CYP to MIP and NIP composite cryogel disc were determined in the concentration range of 1 - 100 μg mL^{-1} and the results were shown in Fig. 7. The calculations of static adsorption capacities of the polymer were based on the following formula:

$$Q = \frac{(C_i - C_f)xV}{m} \quad (5)$$

where, Q (mg g^{-1}) is the mass of α- and β-CYP adsorbed per gram of polymer, C_i (mg L^{-1}) is the initial concentration of α- and β-CYP, C_f (mg L^{-1}) is its final concentration after adsorption, V (L) is the total volume of the adsorption solution, and m (g) is the mass of polymer. The data (Fig.7) indicated the amount of α- and β-CYP bound to the MIP composite cryogel discs was increased along with increased initial concentration till the concentration reached to 50 μg mL^{-1}, the adsorption capacity curve became relatively flat and reached saturation at high α- and β-CYP concentrations. These results indicated that the amount of α- and β-CYP bound to MIP composite cryogel disc was dramatically higher than NIP composite cryogel disc at higher concentrations because of the fact that more specific binding sites of MIP composite cryogel disc were generated at higher concentrations and that was obvious due to imprinting. It seems that during the polymerization process, large population of α- and β-CYP specific binding sites had been produced which were more activated even at higher concentrations of α- and β-CYP.

3.3.3. Scatchard Analysis

The saturation binding data were further processed to generate a Scatchard equation to estimate the binding properties of MIP and NIP composite cryogel disc. The Scatchard equation was as follows:

$$\frac{Q}{[CYP]} = \frac{Q_{max} - Q}{K_D} \quad (6)$$

where Q is the amount of α- and β-CYP bound to polymer at equilibrium, Q_{max} is the apparent maximum adsorption capacity, [CYP] is the free analytical concentration at equilibrium and K_D

is the dissociation constant. The values of K_D and Q_{max} could be calculated from the slope and intercept of the linear curve plotted at $Q/[CYP]$ versus Q.

It was observed that two straight lines were obtained in the case of MIP composite cryogel disc in the plot region of Fig. 8, which indicated that there existed two kinds of binding sites of high and low affinity. The linear regression equations for the left and right slope of the biphasic curves are given in Table 1.

For NIP composite cryogel discs biphasic curve was not observed which reveals that NIP composite cryogel discs only have low affinity binding sites. K_D and Q_{max} were given in Table 1. The adsorption capacity of NIP composite cryogel discs for α- and β-CYP was much lower than that of MIP composite cryogel discs. It hinted that NIP composite cryogel discs did not have the specific adsorption. However, the specific adsorption of MIP composite cryogel discs was achieved and obvious by imprinting.

3.3.4. Langmuir-Freundlich (LF) Isotherm

The MIP and NIP composite cryogel discs were also characterized through LF-isotherm (Fig. 9).

The LF-isotherm equation is as follows [47],

$$B = \frac{N_t a F^m}{1 + a F^m} \tag{7}$$

where B and F are the equilibrium concentrations of bound and free guest in heterogeneous system, respectively. Whereas N_t, a and m are the fitting coefficients and have physical meaning. N_t is the total number of binding sites. The variable 'a' is related to the median binding affinity (K_o) via $K_o = a^{1/m}$ and m is the heterogeneity index. The LF Fitting parameters were calculated from experimental data using solver function in MS Excel using R^2 value to 1 and changing fitting coefficients i.e. N_t, a and m. One of the primary advantages of applying the LF binding model to MIP composite cryogel discs was that binding properties could be readily measured. These parameters enabled direct comparison of the binding parameters of MIP composite cryogel discs even with the polymers that have very different distribution of binding sites. For example comparison of binding parameters of MIP and NIP composite cryogel discs (Table 2)

reveals that MIP composite cryogel discs have higher concentration of binding sites per gram (N_t=96 μmol g^{-1} for α-CYP and 95 μmol g^{-1} for β-CYP). Also MIP composite cryogel is more heterogeneous (m=0.035) as compared to NIP composite cryogel (m=0.3), which is due to imprinting. The accuracy of these values is evaluated with respect to the concentration window in which they were measured. This can be assessed by determining whether K_o falls between the limits $1/F_{min}$ and $1/F_{max}$ and by confirming that the standard errors in the fitting coefficients are not excessively large. These requirements are met in this study (Table 2).

3.4. Binding Specificity of MIP and NIP composite cryogel discs

In order to verify the selectivity of MIP and NIP composite cryogel discs to α- and β-CYP, deltamethrin and permethrin were selected as analogues. The adsorption of MIP and NIP composite cryogel discs to the solutions of α-CYP, β-CYP, deltamethrin and permethrin with concentration of 20 μg mL^{-1} in 20 mL CH_2Cl_2 solution was listed in Table 3.

The specificity of MIP and NIP composite cryogel discs was estimated by the partition coefficients of selected homologues pesticides between polymers and the solution. The partition coefficient K was determined according to the following formula:

$$K = \frac{C_P}{C_S} \tag{8}$$

where C_P was the amount of test analytes bound by MIP and NIP composite cryogel discs, and C_S was the concentration of test analytes remaining in the solution.

Additionally, the imprinting factor (*IF*) and selectivity coefficient (*SC*) were used to evaluate the selectivity properties of MIP and NIP composite cryogel discs toward α- and β-CYP and structurally related pesticides permethrin and deltamethrin. The IF and SC were calculated by the following formula:

$$\text{Imprinting factor } (IF) = \frac{K_i}{K_c} \tag{9}$$

$$\text{Selectivity coefficient } (SC) = \frac{IF_{CYP}}{IF_i} \tag{10}$$

where K_i and K_c represent the partition coefficients of analytes for MIP and NIP composite cryogel discs, IF_{CYP} and IF_i are the imprinting factors for α- and β-CYP and the other two pesticides, respectively.

As shown in Table 3, the bound amount of α- and β-CYP for MIP composite cryogel discs was higher than that of the other two pesticides, suggesting that template molecule had a relatively higher affinity for the imprinted polymer than its analogues. Moreover, the IF of α- and β-CYP were also much higher than those of other homologues. As shown in Fig. 10, α- and β-CYP are isomers of each other and contain same functional groups but permethrin does not contain nitrile group that makes it inappropriate to specific binding sites of MIP composite cryogel discs. In the same way the chlorine atoms are replaced with bromine in deltamethrin that makes it dissimilar from cypermethrin and hence cannot be adsorbed specifically on MIP composite cryogel discs. As α- and β-CYP were used as imprinting templates so at the removal of α- and β-CYP, the complementary cavities in imprinted polymers in the positioning of the functional groups and in the shape of the template were formed. Although the homologues of α- and β-CYP have similar functional groups but the shape and size of α- and β-CYP are different from their homologues and that makes MIP composite cryogel discs specific for α- and β-CYP. The results reveal that imprinted composite cryogels have more affinity for **α- and β-**CYPs as compared to previously reported MIPs [45].

3.5. Solid phase extraction experiments (MISPE)

The synthesized MIP composite cryogel discs were evaluated for sample preparation of α- and β-CYP from water samples aiming at the determination of α- and β-CYP by GC-MS. The pH-dependency of α- and β-CYP adsorption onto the MIP composite cryogel discs was studied in a pH range of 1.0 – 9.0. As shown in Fig. 11 that in all investigated cases, the maximum adsorption was obtained at pH 7.0. At pH values lower and higher than 7.0 the adsorbed amount of α- and β-CYP is relatively lower. However, the adsorption decreases greatly when pH is alkaline.

To optimize volume of sample for MISPE five different volumes 50, 100, 150, 200 and 250 mL of synthetic wastewater (pH 7.0) spiked with 10 μg L^{-1} of α- and β-CYP were checked. It was observed that adsorption increases with increase in volume, it was due to excellent compatibility

of cryogel with aqueous systems. So for convenience in MISPE method 200 mL of samples were adsorbed for rest of the experiments.

In order to optimize the extraction of α- and β-CYP of the sample matrix, blank synthetic wastewater maintained at pH 7 and spiked with 10 μg L^{-1} were used and solvents i.e. ethanol, methanol, acetic acid, acetonitrile and dichloromethane were tested as extraction agents. The highest extraction efficiency (95%) was achieved using methanol. The volume of extraction solvent was also optimized and different volumes i.e. 1, 2, 5 and 10 mL of methanol were tested to extract α- and β-CYP. The maximum extraction was occurred with 2 mL (95%) and remained almost same with 5 mL (95.3%) and 10 mL (95.35%). Thus 5 mL of methanol was used for eluting α- and β-CYP. But the GC-MS method was best optimized with dichloromethane so extract was evaporated till dryness under gentle stream of nitrogen and dissolved again in 0.5 mL of dichloromethane

MISPE was performed by shaking discs in aqueous sample for 20 min. MIP composite cryogel discs did not require step wise activation/conditioning with different solvents, they were simply conditioned with phosphate buffer of pH 7 before adsorption of sample. This is due to the compatability of MIP composite cryogel discs with aqueous environments which is one of the limitations in other MISPE methods based on acrylate backnone MIPs [30, 44, 48].

3.5.1. Validation of MISPE method for extraction of α- and β-CYP

After establishment of the optimal conditions for the retention of α- and β-CYP on the MIP composite cryogel discs, the method for the determination of α- and β-CYP in water samples was validated, using the MISPE procedure on spiked synthetic wastewater followed by GC-MS quantization.

The results were summarized in Table 4. The linear range was between 0.2 to 4 μg L^{-1} with a linearity of 0.999. The limit of detection and quantization were 0.06 and 0.2 μg L^{-1} for α-CYP and 0.1 and 0.3 μg L^{-1} for β-CYP, respectively, established by signal-to-noise ratios of 3 and 10.

The tests of intra- and inter-day precisions produced acceptable relative standard deviation (Table 4).

The validated method was applied to the analysis of lake samples collected from Hacettepe University, Ankara, Turkey. The samples were spiked with three different concentrations (0.3, 1.0 and 4 μg L^{-1}).

3.6. Regeneration and reuse of polymer

Experiments were performed to determine whether the amount of α- and β-CYP adsorbed onto the polymer can be desorbed and it can be regenerated and reused. For this purpose, the MIP composite cryogel discs were used for the adsorption of α- and β-CYP and the same were regenerated and reused. The same process was repeated up to ten consecutive cycles and the results obtained are presented in Fig. 12. The average decrease in adsorption capacity of MIP composite cryogel even after ten adsorption and regeneration cycles was found to be 0.34 and 0.46 mg g^{-1} for α- and β-CYP, respectively. This shows that MIP composite cryogel discs are robust and can be reused several times. Also, method used for the regeneration of polymer is simple. Thus the MIP composite cryogel discs offer brilliant adsorption/desorption properties with excellent kinetics.

4. Conclusion

The results presented here demonstrate that the cryogels embedded with MIP particles can be used for the recognition and selective extraction of α- and β-CYP simultaneously from aqueous systems of environmental importance. The composite cryogel discs embedded with MIP particles specific for α- and β-CYP offered a sensitive, simple and robust MISPE method for the determination of α- and β-CYP using GC-MS. The values of IF reveal that the composite cryogel discs were highly specific for α- and β-CYP and this recognition is accomplished may be through a multistep binding, with the specificity conferred by hydrophobic interactions and shape selectivity. Furthermore, the MIP particles have good site accessibility towards the target α- and β-CYP molecules in aqueous samples because the particles are located, or close to, the macropore surface of cryogel discs. Embedding with MIP particles increased the surface area of the cryogel discs. Moreover, the large surface area of the particles resulted in higher α- and β-CYP binding capacity of the MIP composite cryogel discs. The ability to be reused several times without compromising specificity and adsorption capacity is an additional advantage of composite cryogel discs.

Acknowledgement:

Authors are grateful to TUBITAK (The scientific and technological research council of Turkey) for providing financial support to accomplish this research work.

References

1. I. R. Hill, *Pestic. Sci.,* 1989, **27**, 429-457.
2. J. Velisek, T. Wlasow, P. Gomulka, Z. Svobodova, R. Dobsikova, L. Novotny and M. Dudzik, *Vet. Med-Czech.,* 2006, **51**, 469-476.
3. L. Zhang, X. Gao and P. Liang, *Pestic. Biochem. Phys.,* 2007, **89**, 65-72.
4. S. O. Igbedioh, *Arch. Environ. Health,* 1991, **46**, 218-224.
5. B. E. Hall, J. A. Vickers and J. A. Hopkins, A study to determine the bioaccumulation of 14C-cypermethrin radioactivity in the rat following repeated oral administration 2487-72/20, WHO, 1980.
6. S. Manna, D. Bhattacharyya, T. K. Mandal and S. Das, *J. Vet. Sci.,* 2004, **5**, 241-245.
7. B. Wielgomas and J. Krechniak, *Pol. J. Environ. Stud.,* 2007, **16**, 267-274.
8. F. He, S. Wang, L. Liu, S. Chen, Z. Zhang and J. Sun, *Arch. Toxicol.,* 1989, **63**, 54-58.
9. I. Kakko, T. Toimela and H. Tähti, *Chemosphere*, 2003, **51**, 475-480.
10. D. M. Soderlund and J. R. Bloomquist, *Annu. Rev. Entomol.,* 1989, **34**, 77-96.
11. A. Elbetieha, S. I. Da'as, W. Khamas and H. Darmani, *Arch. Environ. Contam. Toxicol.,* 2001, **41,** 522-528.
12. W. M. Valentine, *Vet. Clin. N. Am-Small,* 1990, **20**, 515-523.
13. S. P. Bhunya and P. C. Pati, *Toxicol. Lett.,* 1988, **41**, 223-230.
14. L. Song, Y.-B. Wang, H. Sun, C. Yuan, X. Hong, J.-H. Qu, J.-W. Zhou and X.-R. Wang, *J. Toxicol. Env. Heal. A*, 2008, **71**, 325-332.
15. H. Rodriguez, C. Tamayo, J. Inostroza, C. Soto, E. Bustos-Obregón and R. Paniagua, *Ecotox. Environ. Safe.,* 2009, **72**, 658-662.
16. B. Giray, A. Gürbay and F. Hincal, *Toxicol. Lett.,* 2001, **118**, 139-146.

17. M. Kale, N. Rathore, S. John and D. Bhatnagar, *Toxicol. Lett.,* 1999, **105**, 197-205.

18. J. Senthil kumar, S. Banudevi, M. Sharmila, P. Murugesan, N. Srinivasan, K. Balasubramanian, M. M. Aruldhas and J. Arunakaran, *Reprod. Toxicol.,* 2004, **19**, 201-208.

19. B. Žegura, T. T. Lah and M. Filipič, *Toxicology*, 2004, **200**, 59-68.

20. H.-P. Li, C.-H. Lin and J.-F. Jen, *Talanta*, 2009, **79**, 466-471.

21. M. B. Woudneh and D. R. Oros, *J. Agr. Food Chem.,* 2006, **54**, 6957-6962.

22. M. D. Gil-García, D. Barranco-Martínez, M. Martínez-Galera and P. Parrilla-Vázquez, *Rapid Commun. Mass Sp.,* 2006, **20**, 2395-2403.

23. F. A. Esteve-Turrillas, A. Pastor and M. d. l. Guardia, *Anal. Chim. Acta,* 2005, **553**, 50-57.

24. E. Van Hoeck, F. David and P. Sandra, *J. Chromatogr. A,* 2007, **1157**, 1-9.

25. Q. Zhou, H. Bai, G. Xie and J. Xiao, *J. Chromatogr. A,* 2008, **1177**, 43-49.

26. V. Casas, M. Llompart, C. García-Jares, R. Cela and T. Dagnac, *J. Chromatogr. A,* 2006, **1124**, 148-156.

27. M. I. Pinto, G. Sontag, R. J. Bernardino and J. P. Noronha, *Microchem. J.,* 2010, **96**, 225-237.

28. S. Lee, J. Gan and J. Kabashima, *J. Agr. Food Chem.,* 2002, **50**, 7194-7198.

29. A. P. Vonderheide, B. Boyd, A. Ryberg, E. Yilmaz, T. E. Hieber, P. E. Kauffman, S. T. Garris and J. N. Morgan, *J. Chromatogr. A,* 2009, **1216**, 4633-4640.

30. X. Shi, J. Liu, A. Sun, D. Li and J. Chen, *J. Chromatogr. A,* 2012, **1227**, 60-66.

31. F. Qiao, H. Sun, H. Yan and K. Row, *Chromatographia*, 2006, **64**, 625-634.

32. A. Ersöz, R. Say and A. Denizli, *Anal. Chim. Acta*, 2004, **502**, 91-97.

33. C. Esen, M. Andac, N. Bereli, R. Say, E. Henden and A. Denizli, *Mater. Sci. Eng. C,* 2009, **29**, 2464-2470.

34. I. N. Savina, C. J. English, R. L. D. Whitby, Y. Zheng, A. Leistner, S. V. Mikhalovsky and A. B. Cundy, *J. Hazard. Mater.,* 2011, **192**, 1002-1008.

35. M. Le Noir, F. Plieva, T. Hey, B. Guieysse and B. Mattiasson, *J. Chromatogr. A,*, 2007, **1154**, 158-164.

36. M. Andaç, G. Baydemir, H. Yavuz and A. Denizli, *J. Mol. Recognit.,* 2012, **25**, 555-563.

37. B. Mattiasson, Advances in Polymer Science, Springer, Switzerland, 2014.

38. S. Asliyuce, L. Uzun, A. Yousefi Rad, S. Unal, R. Say and A. Denizli, *J. Chromatogr. B*, 2012, **889–890**, 95-102.

39. G. Baydemir, M. Andaç, I. Perçin, A. Derazshamshir and A. Denizli, *J. Mol. Recognit.,* 2014, **27**, 528-536.

40. Ş. Öncel, L. Uzun, B. Garipcan and A. Denizli, *Ind. Eng. Chem. Res.,* 2005, **44**, 7049-7056.

41. I. Nopens, C. Capalozza and P. A. Vanrolleghem, University of Gent, Belgium, 2001.

42. K. Yao, S. Shen, J. Yun, L. Wang, F. Chen and X. Yu, *Biochem. Eng. J.,* 2007, **36**, 139-146.

43. K. Yao, J. Yun, S. Shen, L. Wang, X. He and X. Yu, *J. Chromatogr. A,* 2006, **1109**, 103-110.

44. G. Ma and L. Chen, *J. Chromatogr. A,* 2014, **1329**, 1-9.

45. Y. Guo, X. Liang, Y. Wang, Y. Liu, G. Zhu and W. Gui, *J. Appl. Polym. Sci.,* 2013, **128**, 4014-4022.

46. G. Baydemir, N. Bereli, M. Andaç, R. Say, I. Y. Galaev and A. Denizli, *React. Funct. Polym*., 2009, **69**, 36-42.

587 47. F. G. Tamayo, J. L. Casillas and A. Martin-Esteban, *Anal. Chim. Acta,* 2003, **482**, 165-
588 173.

589 48. W.-S. Guan, J.-R. Lei, X. Wang, Y. Zhou, C.-C. Lu and S.-F. Sun, *J. Appl. Polym. Sci*.,
590 2013, **129**, 1952-1958.

591

List of Figures:

614 **List of Tables:**

624

625

626 **Tables**

627 Table 1

	α-CYP	β-CYP
MIP composite cryogel disc		
Linear regression equation for left slope of biphasic curve.	y= 3929.6-417.9x	y= 987.53-178.21x
Correlation coefficient (r) for left slope of biphasic curve.	0.983	0.998
Linear regression equation for right slope of biphasic curve.	y = 248.01-4.8238x	y = 117.61-1.7509x
Correlation coefficient (r) for right slope of biphasic curve	0.96	0.94
K_D (g L^{-1}) from left slope	0.0024	0.006
K_D (g L^{-1}) from right slope	0.21	0.6
Q_{max} (mg g^{-1}) from left slope	9.4	5.54
Q_{max} (mg g^{-1}) from right slope	51.4	67.2
NIP composite cryogel disc		
Linear regression equation	y = 2.0011-0.0871x	y = 1.7902-0.0857x
Correlation coefficient (r)	0.93	0.915
K_D (g L^{-1})	11.5	11.7
Q_{max} (mg g^{-1})	23	21

628

629

630 Table 2

	MIP composite cryogel discs	NIP composite cryogel discs
Fitting coeff. α-CYP		
N_t	96±10μmolg^{-1}	45±7 μmolg^{-1}
a	1.2±0.008 mM^{-1}	2.1±0.07 mM^{-1}
m	0.035±0.005	0.3±0.02
K_o	162 mM^{-1}	14.8 mM^{-1}
Limits of affinity distribution [a]	7.9 – 628327 mM^{-1}	5.25 – 3555 mM^{-1}
Fitting coeff. β-CYP		
N_t	95±12 μmolg^{-1}	43±6 μmolg^{-1}
a	1.2±0.0084 mM^{-1}	2.1±0.07 mM^{-1}
m	0.035±0.005	0.3±0.02
K_o	162 mM^{-1}	17 mM^{-1}
Limits of affinity distribution [a]	7.7 – 339429 mM^{-1}	5.22 – 3533 mM^{-1}
[a] These limits were calculated from the maximum and minimum values of free guest concentration (F_{max} and F_{min}) by the relationships $K_{min} = 1/F_{max}$ and $K_{max} = 1/ F_{min.}$		

631

632 Table 3

Analytes	Q_{MIP} (mg g^{-1})	Q_{NIP} (mg g^{-1})	K_{MIP} (mL g^{-1})	K_{NIP} (mL g^{-1})	*IF*	*SC* α-CYP	*SC* β -CYP
Permethrin	5.35	4.70	0.40	0.30	1.20	9.80	8.40
Deltamethrin	8.25	8.04	0.70	0.67	1.04	11.2	9.60
α-CYP	17.5	7.50	7.00	0.60	11.2	-	-
β-CYP	16.8	6.88	5.25	0.52	10.0	-	-

633

634

635 Table 4

Validation parameters	α-CYP	β-CYP
Linear range (µg L^{-1})	0.2-4	0.3-4
Linearity (R^2)	0.9995	0.9997
Slope (a)	18666828 (±135291)	6381094 (±36536)
Intercept (b)	385429 (±188097)	191335 (±50797)
LOD (µg L^{-1})	0.06	0.1
LOQ (µg L^{-1})	0.2	0.3
Intra-assay precision (% RSD)		
0.3 µg L^{-1} (n = 5)	0.05	0.15
1 µg L^{-1} (n = 5)	0.003	0.08
4 µg L^{-1} (n = 5)	0.001	0.003
Interassay precision (% RSD)		
0.3 µg L^{-1} (n = 3, 3 days)	3.25	2.8
1 µg L^{-1} (n = 3, 3 days)	2.2	1.75
4 µg L^{-1} (n = 3, 3 days)	0.75	0.5
Accuracy (% recovery) Lake Water		
0.3 µg L^{-1} (n = 3)	92	91.5
1 µg L^{-1} (n =3)	95	95.3
4 µg L^{-1} (n = 3)	98	97.5

636

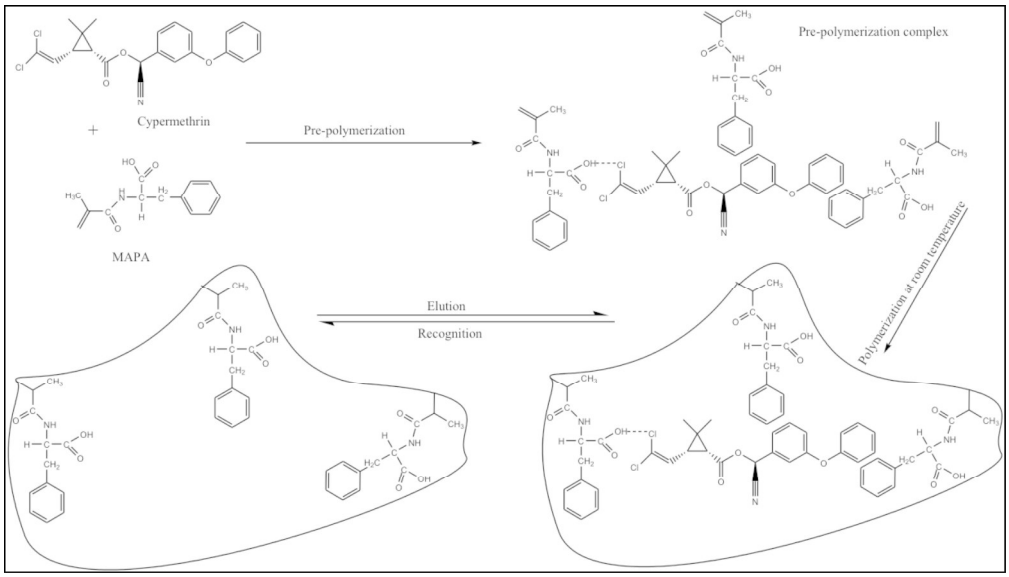

Fig. 1. Schematic representation of imprinting of cypermethrin in poly (hydroxyethyl methacrylate- N-methacryloyl-L-phenylalanine) particles.
404x228mm (300 x 300 DPI)

Fig. 2. MIP composite cryogel discs.
140x78mm (300 x 300 DPI)

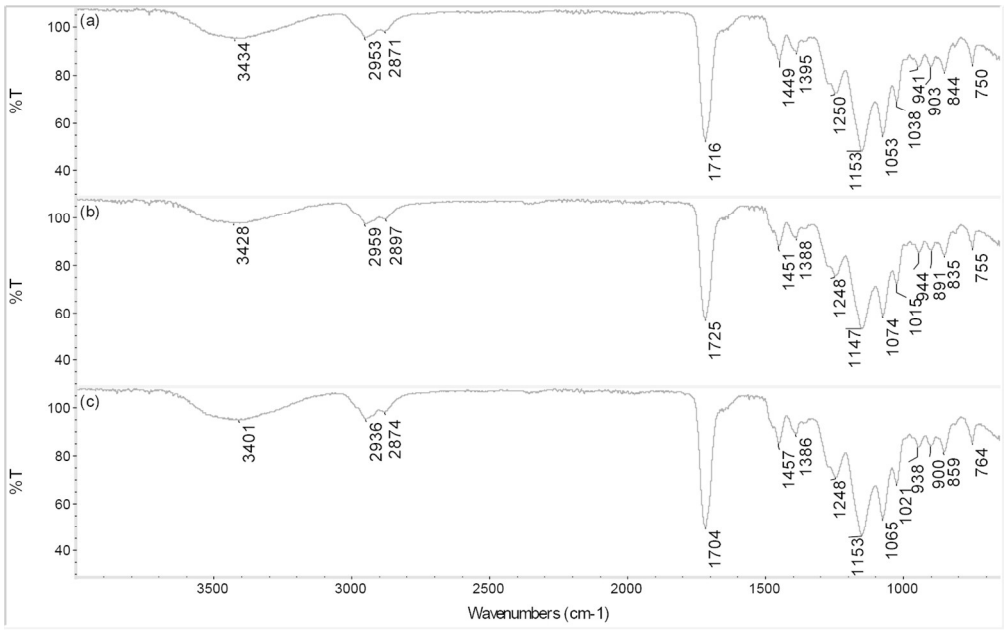

Fig. 3. FT-IR spectra of (a) α-CYP imprinted particles (b) β-CYP imprinted particles (c) non-imprinted (NIP) particles.
127x79mm (300 x 300 DPI)

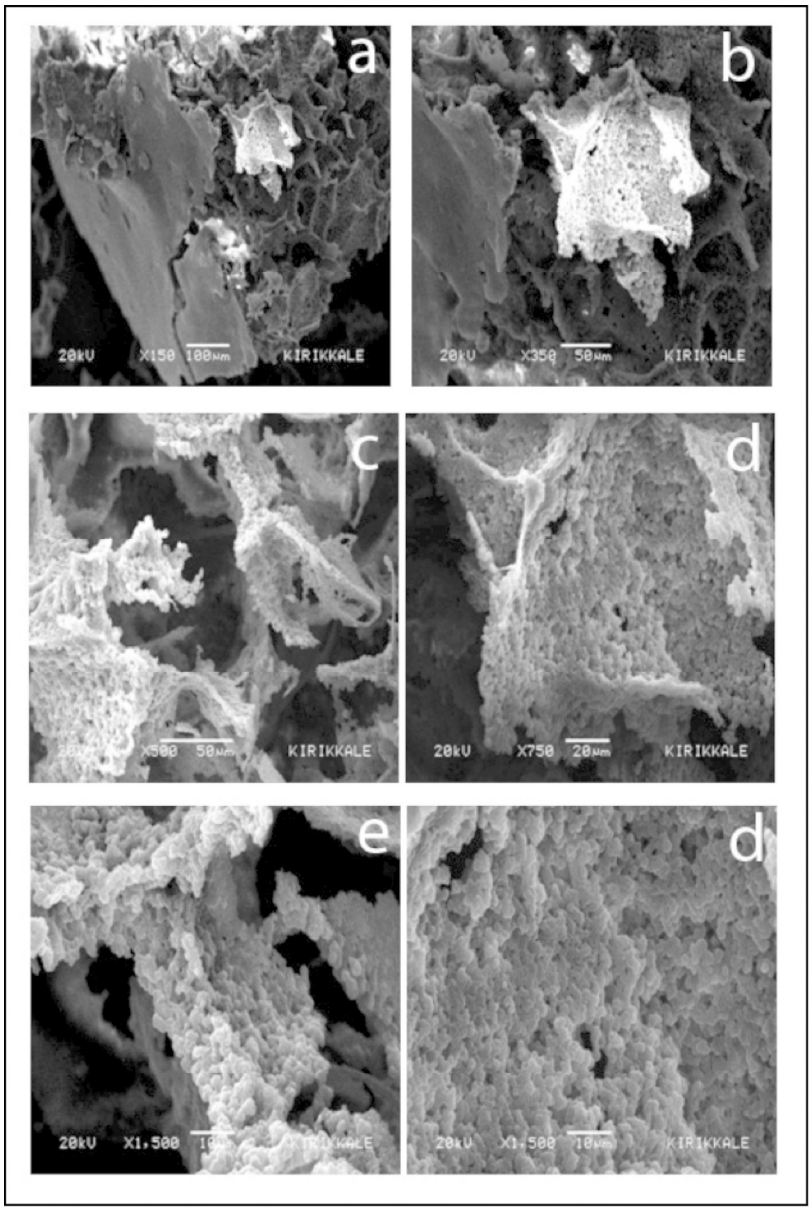

Fig. 4. SEM images of MIP composite cryogel discs.
170x254mm (300 x 300 DPI)

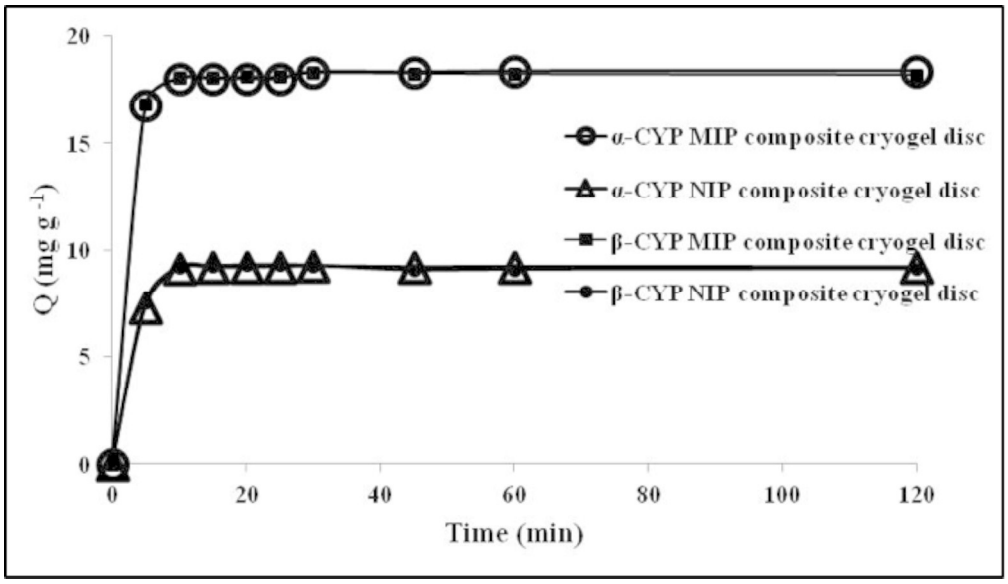

Fig. 5. Uptake kinetics plots of MIP and NIP composite cryogel discs for adsorption of α- and β-CYP.
221x127mm (300 x 300 DPI)

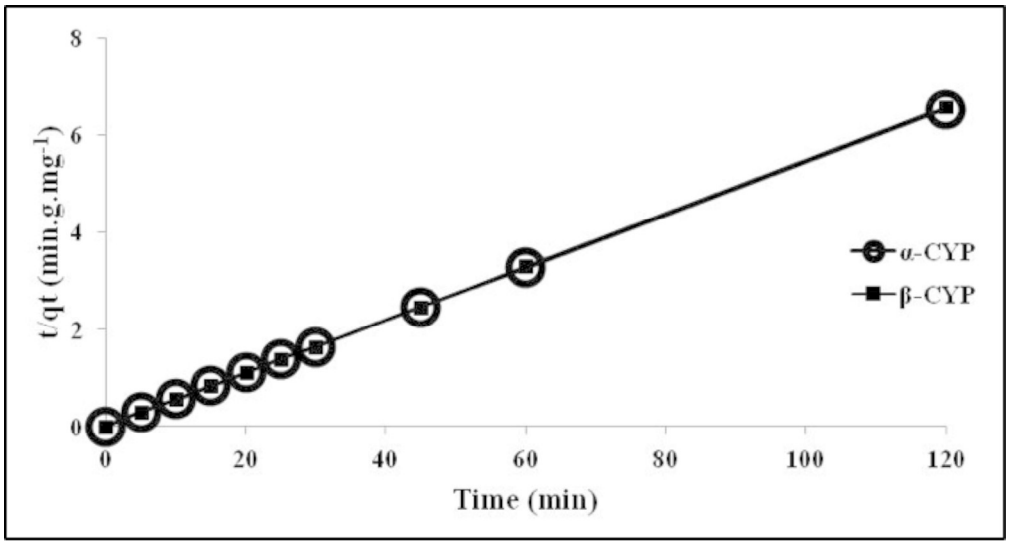

Fig. 6. Pseudo-second order kinetic model of MIP composite cryogel discs for adsorption of α- and β-CYP.
237x127mm (300 x 300 DPI)

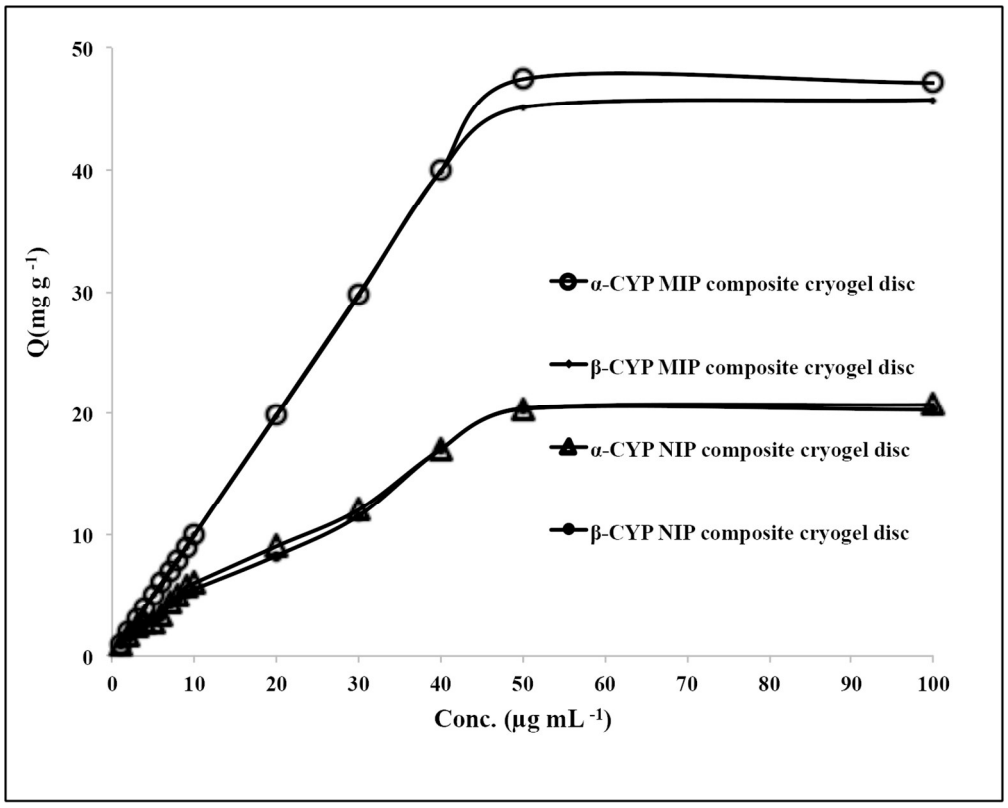

Fig. 7. Adsorption isotherms of MIP and NIP composite cryogel discs for α- and β-CYP in methanol.
127x101mm (300 x 300 DPI)

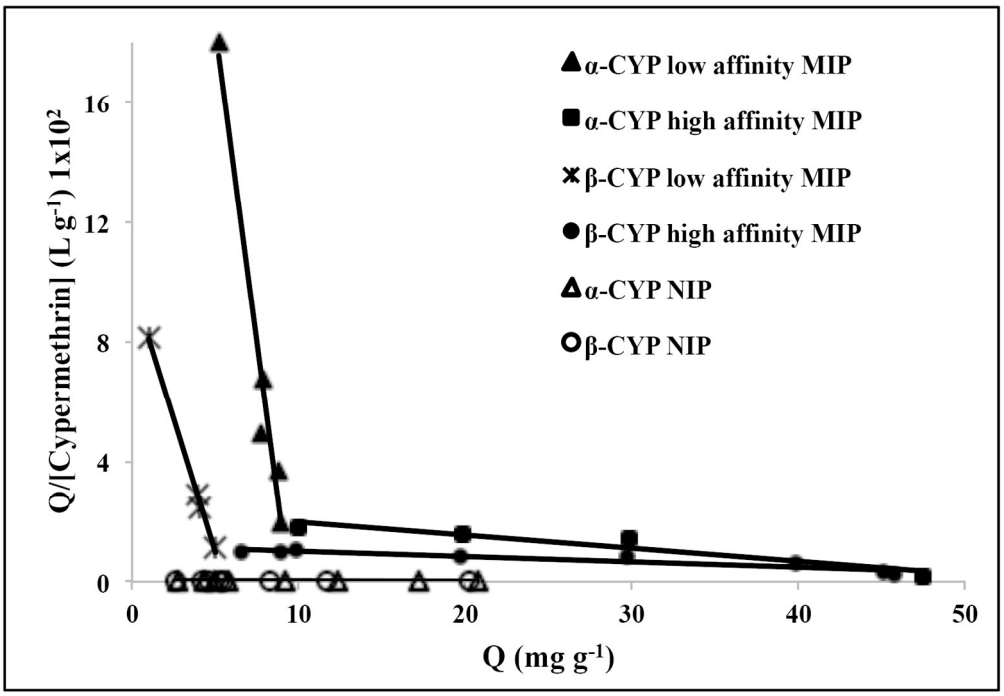

Fig. 8. The scatchard plot to estimate the binding nature of MIP and NIP composite cryogel discs.
147x101mm (300 x 300 DPI)

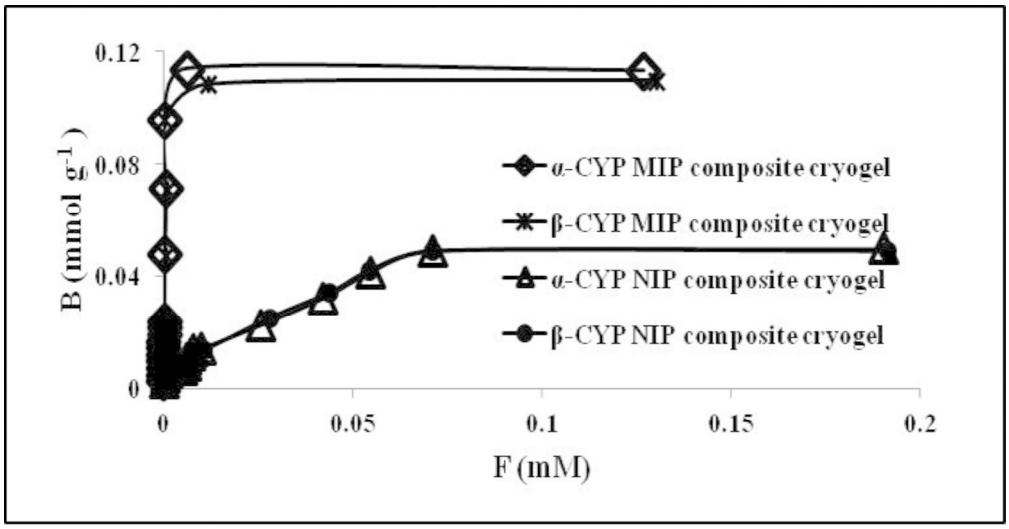

Fig. 9. Binding isotherm of MIP and NIP composite cryogel discs for α- and β-CYP fitted to Langmuir-Freundlich (LF) isotherm.
177x92mm (300 x 300 DPI)

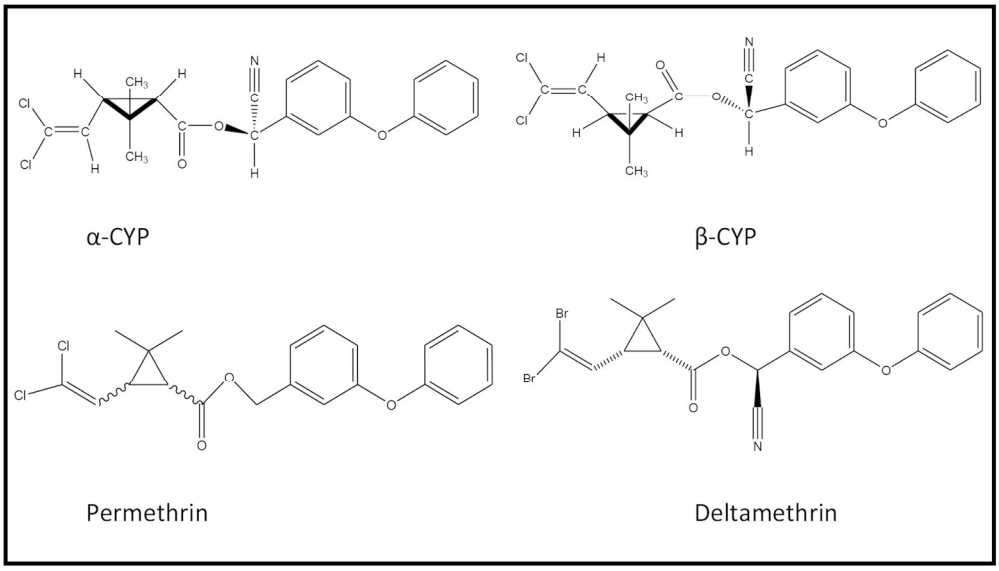

Fig. 10. Chemical structures of related pyrethroid pesticides used in this study.
178x101mm (300 x 300 DPI)

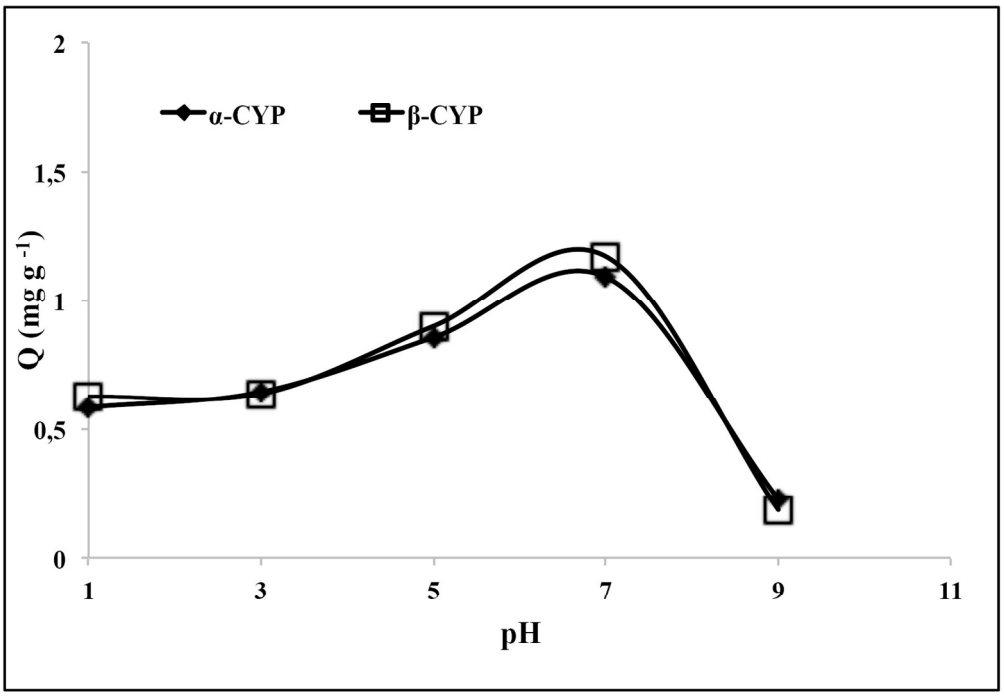

Fig. 11. Adsorption of MIP and NIP composite cryogel discs for α- and β-CYP at different pH.
147x101mm (300 x 300 DPI)

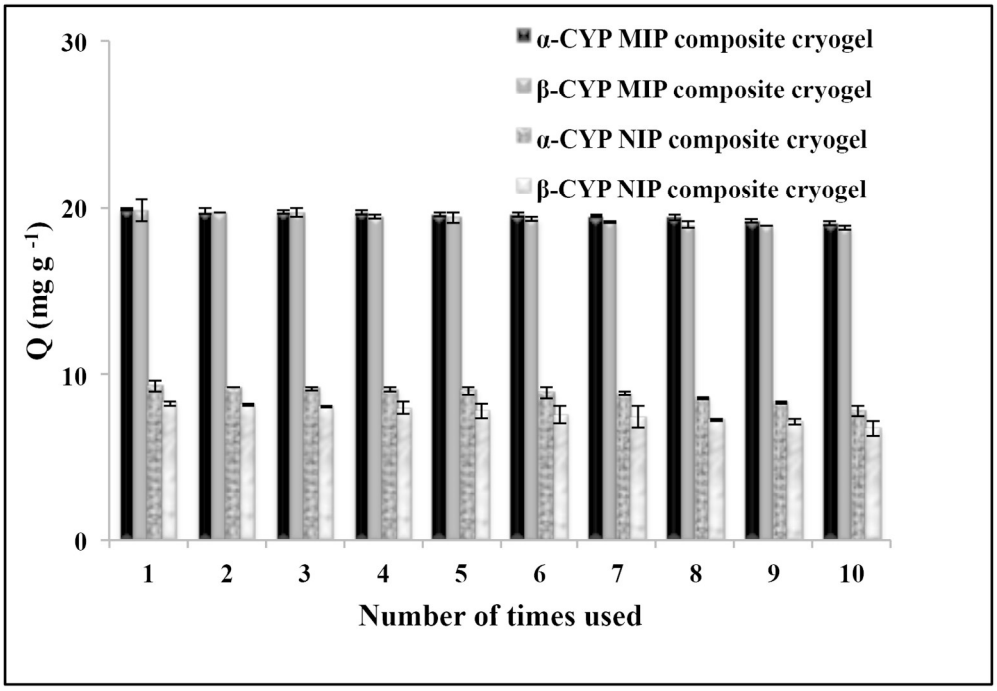

Fig. 12. Reuse of MIP and NIP composite cryogel discs.
142x99mm (300 x 300 DPI)